

Optical properties of human colon tissues in the 350–2500 nm spectral range

A.N. Bashkatov, E.A. Genina, V.I. Kochubey, V.S. Rubtsov, E.A. Kolesnikova, V.V. Tuchin

Abstract. We present the optical characteristics of the mucosa and submucosa of human colon tissue. The experiments are performed *in vitro* using a LAMBDA 950 spectrophotometer in the 350–2500 nm spectral range. The absorption and scattering coefficients and the scattering anisotropy factor are calculated based on the measured diffuse reflectance and total and collimated transmittance spectra using the inverse Monte Carlo method.

Keywords: *integrating sphere spectrophotometry, inverse Monte Carlo method, mucous membrane, submucous membrane, absorption coefficient, scattering coefficient, reduced scattering coefficient, scattering anisotropy factor.*

1. Introduction

Knowledge of the optical characteristics of tissues is one of the key issues in the development of mathematical models that adequately describe the propagation of light in biological tissues, which in turn is crucial for the development of new optical methods used in various fields of biology and medicine [1, 2]. At the same time, in spite of a considerable number of papers devoted to the determination of optical parameters of biological tissues [1–10], their optical properties in a wide wavelength range are currently poorly studied, even though the analysis of visible and near-IR radiation absorption by biological tissues is crucial to the development of the methods of optical diagnosis, endoscopic surgery, photodynamic and photothermal therapy of various diseases, including cancer.

A key issue in the prevention of colon cancer is the diagnosis and treatment of pre-cancer [11–13]. Unfortunately, despite the undoubted social significance of the problem, laser scalpels in surgical endoscopy of the colon have not found wide application yet. In particular, this is due to the

lack of science-based criteria, which would allow endoscopists and laser surgical instrument developers to use an optimal laser wavelength for surgery [13] and to choose the most suitable type of laser, respectively.

One of the criteria on which this selection can be done is an objective analysis of the optical characteristics of colon tissue. Previously, they were studied in papers [14–19]. However, the investigation of the optical characteristics was performed only in the visible wavelength range (360–685 nm) [14]; in the ranges of 400–1100 nm [15], 300–700 nm [16], 300–800 nm [17]; and only at particular wavelengths (850, 980 and 1060 nm [18], 476.5, 488, 496.5, 514.5, 532 nm [19]). At the same time, the rapid development of laser technology and the consequent emergence of new types of lasers require the determination of the optical characteristics of tissues in a much broader range of wavelengths. In addition, the authors of all the above papers investigated the optical properties of the entire biological tissue on the whole rather than separate layers.

In light of the above, the purpose of this paper is to measure the optical properties of mucous and submucous membranes of the human colon in the 350–2500 nm spectral range.

2. Materials and methods

In the study we used 20 samples of human colon tissue (10 samples of the mucosa and 10 samples of the submucosa) taken from different 40-to-60-year-old patients in the course of routine operations or histological sectioning. Immediately after surgery or autopsy the tissue samples were placed in a 0.9% aqueous solution of NaCl and stored therein prior to the spectral measurements for 8–12 h at a temperature of 4 °C. The area of each sample was 500–600 mm². To measure the thickness, the samples were placed between two glass slides; measurements were performed with a micrometer at several points. The average thickness of the samples was 0.56 ± 0.41 mm with a ± 50 μ m accuracy of each measurement.

The optical properties of biological tissues were investigated in the 350–2500 nm spectral range using a LAMBDA 950 integrating sphere spectrophotometer (PerkinElmer, USA), which is a two-channel diffraction monochromator having an integrated control and signal registration system. The size of the light beam incident on the sample during the measurement of diffuse reflectance and total transmittance was 1 × 4 mm, and the scanning speed was 5 mm s⁻¹. To measure collimated transmittance we used a specially designed add-on device, which consisted of a holder to fix the sample of biological tissue and a system of four diaphragms (Fig. 1) with a diameter of 2 mm each. All measurements were performed at room temperature (~20 °C).

A.N. Bashkatov, E.A. Genina, V.I. Kochubey, E.A. Kolesnikova
N.G. Chernyshevsky Saratov State University, ul. Astrakhanskaya 83, 410012 Saratov, Russia; e-mail: anbashkatov@mail.ru, eagenina@yandex.ru, saratov_gu@mail.ru, ekaterina.a.kolesnikova@mail.ru;

B.S. Rubtsov V.I. Razumovsky Saratov State Medical University, ul. Bol'shaya Kazach'ya 112, 410012 Saratov, Russia; e-mail: rubzov999@yandex.ru;

V.V. Tuchin N.G. Chernyshevsky Saratov State University, ul. Astrakhanskaya 83, 410012 Saratov, Russia; Institute of Precision Mechanics and Control, Russian Academy of Sciences, ul. Rabochaya 24, 410028 Saratov, Russia; University of Oulu, 90014, Oulu, P.O. Box 4500, Finland; e-mail: tuchinvv@mail.ru

Received 7 July 2014

Kvantovaya Elektronika 44 (8) 779–784 (2014)

Translated by I.A. Ulitkin

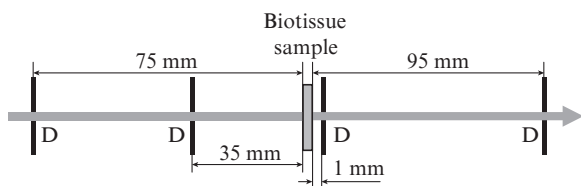


Figure 1. Scheme of the add-on device for measuring collimated transmittance of samples of biological tissue; D is a $\varnothing 2$ mm diaphragm.

For the results of the experiments to be processed and the optical parameters of the mucous membrane to be determined, we used a combined method, the first stage of which involved the measurement data handling using the inverse adding-doubling method [20]. Then, the resulting values of the coefficients of absorption μ_a , scattering μ_s and scattering anisotropy factor g were refined using the inverse Monte Carlo (IMC) method by minimising the target function

$$F(\mu_a, \mu_s, g) = [R_d^{\text{exp}} - R_d^{\text{calc}}(\mu_a, \mu_s, g)]^2 + [T_c^{\text{exp}} - T_c^{\text{calc}}(\mu_a, \mu_s, g)]^2 + [T_t^{\text{exp}} - T_t^{\text{calc}}(\mu_a, \mu_s, g)]^2$$

with the boundary conditions $0 \leq g \leq 0.99$. Here, R_d^{exp} , T_t^{exp} , T_c^{exp} , R_d^{calc} , T_t^{calc} and T_c^{calc} are diffuse reflectances and total and collimated transmittances experimentally measured and theoretically calculated by the Monte Carlo (MC) method [21], taking into account the geometry of the medium under study and the experiment. As a minimisation procedure we used the Nelder–Mead simplex method described in detail elsewhere [22]. The iterative procedure continued until the measured and calculated data were matched with a given accuracy (less than 0.1%). Figure 2 shows a block diagram of the method used.

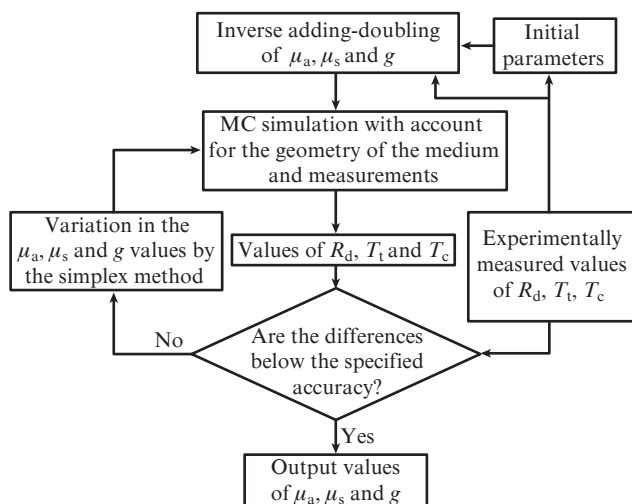


Figure 2. Block diagram of the method used for determining the optical parameters of biological tissues.

As the initial values of μ_a , μ_s and g in the block of the initial parameters, we used the solutions to the system of equations (1)–(3) [20]:

$$\frac{\mu_s'}{\mu_a + \mu_s'} = \begin{cases} 1 - \left(\frac{1 - 4R_d^{\text{exp}} - T_t^{\text{exp}}}{1 - T_t^{\text{exp}}} \right)^2, & \text{если } \frac{R_d^{\text{exp}}}{1 - T_t^{\text{exp}}} < 0.1 \\ 1 - \frac{4}{9} \left(\frac{1 - R_d^{\text{exp}} - T_t^{\text{exp}}}{1 - T_t^{\text{exp}}} \right)^2, & \text{если } \frac{R_d^{\text{exp}}}{1 - T_t^{\text{exp}}} \geq 0.1 \end{cases}, \quad (1)$$

$$(\mu_a + \mu_s')l = \begin{cases} -\frac{\ln T_t^{\text{exp}} \ln 0.05}{\ln R_d^{\text{exp}}}, & \text{если } R_d^{\text{exp}} \leq 0.1, \\ 2^{1+5(R_d^{\text{exp}} + T_t^{\text{exp}})}, & \text{если } R_d^{\text{exp}} > 0.1, \end{cases} \quad (2)$$

$$\mu_t = -\ln(T_c^{\text{exp}})/l, \quad (3)$$

where $\mu_t = \mu_a + \mu_s$ is the attenuation coefficient (cm^{-1}); $\mu_s' = \mu_s(1 - g)$ is the reduced scattering coefficient (cm^{-1}); and l is the thickness of the measured sample of biological tissue (cm).

In the block of the initial parameters we set the sample and measurement geometry, the parameters of the integrating sphere, etc. After the introduction of the initial parameters, the experimental data were processed by the inverse adding-doubling method, the main purpose of which is to obtain a more accurate initial approximation. Since the main drawback of the IMC method is a high computational burden, the use of the inverse adding-doubling method at the first stage can significantly minimise this parameter and significantly reduce the computational time of the optical parameters of tissues.

At the next stage we performed MC simulation of diffuse reflectances and total and collimated transmittances, taking into account the real geometry of a biological tissue sample and measurements, and compared the calculated values with the experimentally measured values of R_d , T_t and T_c . The given accuracy having been reached, the process stopped and the calculated values of μ_a , μ_s and g were written in a file. If the difference between the experimentally measured and theoretically calculated values of R_d , T_t and T_c was higher than the initially specified computational accuracy, we used the simplex method to modify the value of μ_a , μ_s and g . Then, the process was repeated until the required accuracy of matching the experimental and calculated values of R_d , T_t and T_c was achieved.

3. Results and discussion

Figures 3–6 show the absorption and scattering spectra of colon wall tissue, calculated by the IMC method based on the experimental values of the coefficients R_d^{exp} , T_t^{exp} and T_c^{exp} . The absorption spectra of the mucosa and submucosa were obtained in the 350–2500 nm spectral range (Fig. 3). The vertical lines in Figs 3–6 correspond to the standard deviation calculated by the formula

$$SD = \left(\sum_{i=1}^N (\bar{\mu}_a - \mu_{ai})^2 / [N(N-1)] \right)^{1/2},$$

where $N = 10$ is the number of measured samples of the mucosa or submucosa; μ_{ai} is the absorption coefficient of the i th sample of biological tissue; and $\bar{\mu}_a = \sum_{i=1}^N \mu_{ai} / N$ is the average value of the absorption coefficient at each spectral point. The spectrum in Fig. 3 has clearly visible absorption bands of water with maxima at 1185, 1450 and 1945 nm [23, 24] and of haemoglobin with maxima at 410, 545 and 575 nm [25]. The absorption bands of water with maxima at 975 and 1785 nm are much less pronounced. The observed increase in absorption in the region over 2200 nm is a short-wavelength arm of

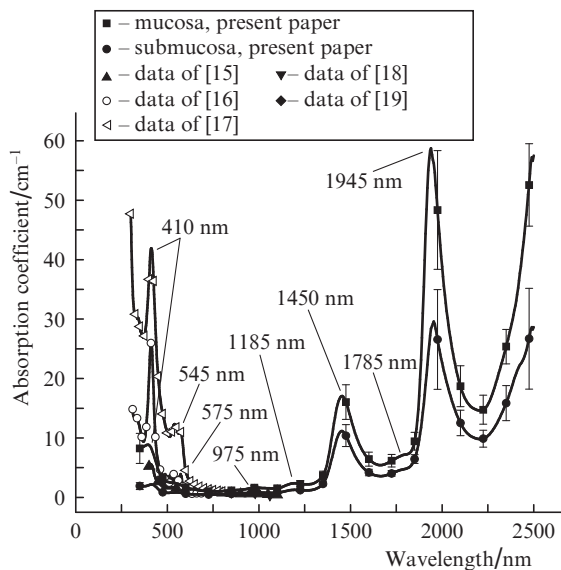


Figure 3. Absorption coefficient of human colon tissue.

the absorption band of water with a maximum at 2950 nm [23, 24]. The increase in the standard deviation of the absorption coefficient, observed in the absorption bands, indicates a different content of water and haemoglobin in different samples of biological tissue.

For comparison, Fig. 3 shows the experimental data presented in [15–19]. One can see that they and our data agree quite well, except for the results presented in [16, 17] for the blue-green region of the spectrum. These differences are due to the use of different methods of experimental data processing. Thus, the optical characteristics in [16] were reconstructed using the Kubelka–Munk method [26, 27], and in [17] – using the one-dimensional solution to the equation of radiative transfer in the diffusion approximation [28]. Since the methods [26–28] are approximate ones for solving the radiative transfer equation, their use for the processing of the experimental data apparently leads to the observed differences in the values of the absorption coefficients obtained in this work and in [16, 17].

Comparison of the absorption spectra of the mucosa and submucosa shows that the absorption in the mucous membrane is higher than that in the submucous one. This is particularly noticeable in the spectral region from 1000 nm to 2500 nm. The difference is mainly due to higher water content (the main chromophore of the tissue under study in this spectral region) in the mucosa compared with the submucosa [29]. In addition, there is an optical mechanism of enhancement of the absorption due to multiple scattering. As a rule, for the light propagation in biological tissues to be analysed, use is made of statistical modelling based on the discrete representation of photons and description of the processes of multiple scattering and absorption by the MC method. Under this approach, the fundamental difference between a weakly and a strongly scattering medium is that in the second case, the mean free path of photons between the interactions with the structural elements of biological tissue that are responsible for the absorption of photons, is significantly less than in the first case. Therefore, as a result of overexposure of absorbing centres by multiply scattered photons, the fraction of absorbed photons in a strongly scattering medium can, *ceteris paribus*, be greater than in a weakly scattering medium with

the same amount of absorbing particles due to an increase in the number of interactions. The above-described mechanism of enhancement of the absorption due to multiple scattering was previously discussed with reference to problems photothermal therapy [30], and computer simulations performed in this work qualitatively confirmed the contribution of multiple scattering to an increase in the absorption. As seen from Figs 4 and 5, the scattering in the mucosa prevails over the scattering in the submucosa. This fact is responsible, in combination with higher water content, for a stronger absorption in the mucous membrane (see Fig. 3).

Figure 4 shows the spectra of the reduced scattering coefficient of the mucosa and submucosa of the colon wall, which were obtained by averaging the spectra measured for each of the 20 samples of biological tissue. It is clearly seen that in the region from 350 to 1300 nm, the reduced scattering coefficient gradually decreases towards longer wavelengths, which is on the whole consistent with the general character of the spectral behaviour of the scattering characteristics of biological tissues. However, starting from 1300 nm, when the wavelength is increased, the spectral behaviour of the reduced scattering coefficient becomes diametrically opposite and we observe a deviation from the monotonic dependence in the region of the absorption bands.

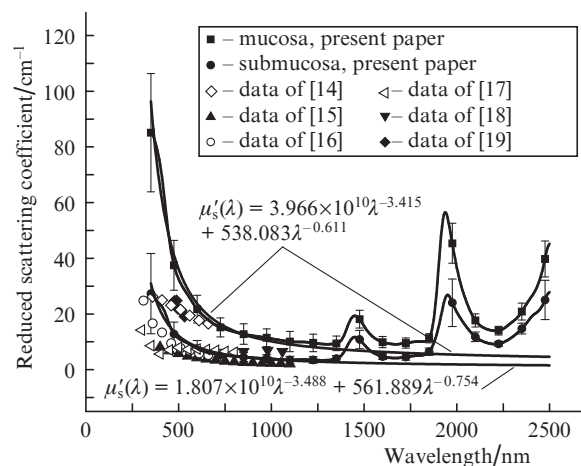


Figure 4. Reduced scattering coefficient of human colon tissue.

The deviation of the spectral dependence of the scattering characteristics from the monotonic dependence is explained by an increased influence of the imaginary part of the complex refractive index of the scattering centres (collagen fibres in this case) in the region of the absorption bands. According to the Mie theory, the scattered light intensity is mainly determined by the complex refractive index of the scatterers of biological tissue [31], and the growth of the imaginary part of the complex refractive index in the region of the absorption bands leads to a change in the scattering cross section and in the reduced scattering coefficient in this spectral region. The increase in the imaginary part of the complex refractive index of the scatterers causes a significant decrease in scattering anisotropy factor g , which, along with the scattering coefficient μ_s of biological tissue, generates the spectrum of the reduced scattering coefficient $\mu_s' = \mu_s(1 - g)$.

The authors of [32, 33] have previously shown experimentally that in the region of the absorption bands of water with maxima at 1450 and 1945 nm, g decreases. This inevitably

leads to an increase in μ'_s and the appearance of bands in its spectrum, a decrease in scattering anisotropy factor in the absorption bands being proportional to the intensity of the absorption bands. The authors of [34, 35] developed a theory and built a computer model to explain this behaviour of the reduced scattering coefficient spectrum. The data presented in Fig. 4 are in good agreement with those mentioned above. In the 350–1300 nm region, the absorption of water is either insignificant or the absorption bands are characterised by low intensities (see Fig. 3 and the data of [23, 24]). Therefore, the formation of the μ'_s spectrum in this region is mainly determined by the real part of the complex refractive index, and the μ'_s spectrum decreases rather monotonically towards longer wavelengths. In the 1300–2500 nm region, the absorption spectrum demonstrates sufficiently strong absorption bands of water, and so the formation of the spectrum is influenced not only by the real but also by the imaginary part of the complex refractive index of the scattering centres of biological tissue, which is manifested as an increase in light scattering in this spectral region with sufficiently strong peaks in the region of the absorption bands.

Comparison of our data with those presented in [14–19] shows a fairly good agreement between them (see Fig. 4). At the same time, one can clearly see that the data from [14, 19] lie in the range between the values of μ'_s for the mucosa and submucous membranes, and the data from [15–18] are lower than the values of μ'_s for the submucous membrane, which is due to differences in the methods of storage and preparation of the samples for spectral measurements. Firstly, in all the previous studies [14–19], measurements were carried out without separating the mucosa and submucosa of colon tissues. In addition, when preparing samples [15, 16, 18], they were subjected to deep freezing at temperatures from 203 [15] to 77 K [18], and in the latter case, the samples were homogenised. It is obvious that deep freezing and homogenisation of tissue samples resulted in a change of the scattering characteristics. This is apparently the main reason for the observed differences between our data and the data presented in [15, 16, 18]. In the blue region of the spectrum, the differences between our results and those of [17] are caused by the use of a one-dimensional solution to the equation of radiative transfer in the diffusion approximation [28] in the course of processing, which apparently led to a significant overestimation of the absorption coefficient and an underestimation of the reduced scattering coefficient. Our results of measurements and the data from [14, 19] (see Fig. 4) are in good agreement. Because the authors of [14, 19] did not separate the mucosa and submucosa, the averaging of the μ'_s values for the mucosa and submucosa give a better agreement with the data from [14, 19].

As was shown in papers [1–3, 5, 7, 36–40], in the visible and near-IR spectra the dependence of both the scattering coefficient and the reduced scattering coefficient is approximated with good accuracy by a power function of the wavelength λ , which has the form: $\mu_s(\lambda) = a\lambda^{-w}$, where the parameter a is determined by the concentration of the scattering centres of biological tissue and the ratio of the refractive indices of the scatterers and their surrounding medium, and the parameter w (wavelength exponent) characterises the average size of the scatterers and determines the spectral behaviour of the scattering coefficient. Figure 4 shows the approximations of the spectra of the reduced scattering coefficients of the mucous and submucous membranes by the functions $\mu'_s(\lambda) = 3.966 \times 10^{10} \lambda^{-3.415} + 538.083 \lambda^{-0.611}$ and $\mu'_s(\lambda) = 1.807 \times 10^{10} \lambda^{-3.488} + 561.889 \lambda^{-0.754}$, respectively, where λ is taken in nano-

metres. It is seen that these functions well approximate the experimental data in the 350–1300 nm spectral range, as opposed to the 1300–2500 nm spectral range demonstrating their discrepancy. The fact that the approximating functions are a combination of two power functions indicates the formation of the spectrum of the reduced scattering coefficient by at least two types of scatterers. The first term of the approximating function is responsible for the scattering of light caused by small enough (though not Rayleigh ones with $w = 4$) scatterers, such as mitochondria of cells, some collagen fibres, etc. The second term corresponds to sufficiently large scatterers (Mie scatterers), such as fibre bundles or their plexus as well as cell membranes or other sufficiently large components of epithelial cells.

Comparison of the functions approximating the μ'_s spectra of the mucous and submucous membranes indicates that the effective sizes of the scatterers of these types of tissues are virtually equal. At the same time it is clear that when compared to the submucosa, the mucous membrane comprises a larger number of small scatterers, which is in full accord with the structural features of biological tissues in question.

Figure 5 shows the spectra of the scattering coefficients of the mucosa and submucosa of the human colon wall, which were obtained by averaging the corresponding spectra measured for each of 20 samples of biological tissue. It is clearly seen that in the 350–1800 nm region, the scattering coefficient gradually decreases towards longer wavelengths, which on the whole corresponds to the general character of the spectral behaviour of the scattering characteristics of the tissues. However, starting from 1800 nm, the increase in the wavelength is accompanied by an increase in the scattering coefficient and the appearance of peaks in the absorption bands of water, which is explained by the increasing influence of the imaginary part of the complex refractive index of the scattering centres in this region.

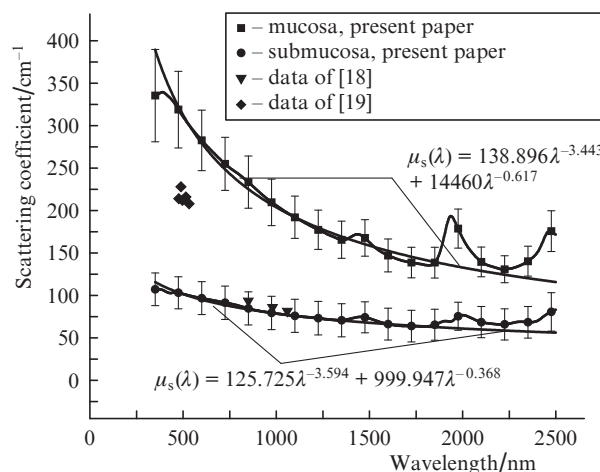


Figure 5. Scattering coefficient of human colon tissue.

One can see from Fig. 5 that the values of the scattering coefficient [19] lie in the range between the values of the scattering coefficient we measured for the mucous and submucous membranes, because the authors [19] did not separate the scattering characteristics of the mucosa and submucosa. The averaging of the values of the scattering coefficient for

the mucosa and submucosa will provide good agreement with the results of [19]. The data presented in [18] are almost identical with our values of the scattering coefficient for the submucosa, which is apparently due to very deep freezing and homogenisation of tissue samples made in [18].

Figure 5 shows the approximations of the spectral dependences of the scattering coefficient of the mucosa and submucosa by the functions $\mu_s(\lambda) = 138.896\lambda^{-3.443} + 14460\lambda^{-0.617}$ и $\mu_s(\lambda) = 125.725\lambda^{-3.594} + 999.947\lambda^{-0.368}$, respectively. It can be seen that these functions well approximate the experimental data in the 350–1800 nm spectral range, and in the 1800–2500 nm range we observe a discrepancy between the experimental results and the approximating dependence. As in the case of μ'_s , the approximating functions are a combination of two power functions, indicating the formation of the scattering coefficient spectrum by at least two types of scatterers.

Figure 6 shows the spectral dependences of the scattering anisotropy factor of the mucous and submucous membranes of the colon tissues and their approximation by the function $g(\lambda) = 0.77 + 0.18[1 - \exp(-(\lambda - 378.7)/111.1)]$ and $g(\lambda) = 0.77 + 0.19[1 - \exp(-(\lambda - 380.4)/128.1)]$, respectively. The experimental data in the 350–1300 nm region are well approximated by these functions, and the analysis carried out in [5, 6] suggests that in the visible region the shape of the scattering anisotropy spectrum is influenced by both small and large particles, while in the near-IR region the main contribution is made only by large enough scatterers, as evidenced by the growth of g with increasing λ . In the 1300–2500 nm spectral region, we observe a significant decrease in g with sharp dips in the absorption bands of water, which is explained by the influence of the imaginary part of the complex refractive index of the scatterers and their surrounding medium.

One can see from Fig. 6 that in the 350–1300 nm region the spectral dependences of the scattering anisotropy factor of the mucosa and submucosa almost coincide with each other, which confirms the conclusion (made previously by analysing the spectra of the reduced scattering coefficient) about the proximity of the effective size of the mucosa and submucosa scatterers. The experimental data of [18, 19] pre-

sented in Fig. 6 are in good agreement with those obtained in the present work.

4. Conclusions

Development of the methods of laser surgery requires knowledge of the optical characteristics of biological tissues in a wide range of wavelengths. In this study, we have studied experimentally the optical parameters of the mucosa and submucosa of human colon tissue. The experiments have been performed *in vitro* using a LAMBDA 950 spectrophotometer in the 350–2500 nm spectral range. By using the experimentally measured spectra of diffuse reflectance and total and collimated transmittance with the help of the inverse MC method, we have calculated for the first time the absorption and scattering spectra of the mucosa and submucosa.

The results obtained can be used to develop new and to optimise existing surgical techniques of gastrointestinal endoscopy of various diseases.

Acknowledgements. The study was supported by the Russian Science Foundation (Project No. 14-15-00186).

References

1. Tuchin V.V. *Tissue Optics. Light Scattering Methods and Instruments for Medical Diagnosis* (Bellingham, SPIE Press, 2007; Moscow: Fizmatlit, 2012).
2. Tuchin V.V. *Lazery i volokonnaya optika v biomeditsinskikh issledovaniyakh* (Lasers and Fibre Optics in Biomedical Research) (Moscow: Fizmatlit, 2010).
3. Bashkatov A.N., Genina E.A., Tuchin V.V., in *Handbook of Biomedical Optics*. Ed. by D.A. Boas, C. Pitris, N. Ramanujam (Boca Raton, London, New York: CRC Press Taylor & Francis Group, 2011) Ch. 5, p. 67.
4. Bashkatov A.N., Genina E.A., Kochubey V.I., Tuchin V.V., Chikina E.E., Knyazev A.B., Mareev O.V. *Opt. Spektrosk.*, **97**, 1043 (2004).
5. Bashkatov A.N., Genina E.A., Kochubey V.I., Tuchin V.V. *J. Phys. D: Appl. Phys.*, **38**, 2543 (2005).
6. Bashkatov A.N., Genina E.A., Kochubey V.I., Gavrilova A.A., Kapralov S.V., Grishaev V.A., Tuchin V.V. *Med. Laser Appl.*, **22**, 95 (2007).
7. Bashkatov A.N., Genina E.A., Tuchin V.V. *J. Innovative Optical Health Sci.*, **4**, 9 (2011).
8. Cheong W.-F., Prahl S.A., Welch A.J. *IEEE J. Quantum Electron.*, **26**, 2166 (1990).
9. Mobley J., Vo-Dinh T., in *Biomedical Photonics Handbook*. Ed. by T. Vo-Dinh (Boca Raton, London, New York: CRC Press LLC, 2003) Ch. 2.
10. Jacques S.L. *Phys. Med. Biol.*, **58**, R37 (2013).
11. Zaikin S.I. *Cand. Diss.* (Kemerovo, KemGMA, 2009).
12. Farraye F.A., Wallace M. *Gastrointestinal Endoscopy Clinics of North America*, **12**, 41 (2002).
13. Rubtsov V.S., Chalyk Yu.V. *Russ. Zh. Gastroenterol. Hepatol. Koloproktol.*, **3**, 86 (2011).
14. Zonios G., Perelman L.T., Backman V., Manoharan R., Fitzmaurice M., van Dam J., Feld M.S. *Appl. Opt.*, **38**, 6628 (1999).
15. Ao H., Xing D., Wei H., Gu H., Wu G., Lu J. *Phys. Med. Biol.*, **53**, 2197 (2008).
16. Zonios G., Cothren R.M., Arendt J.T., Wu J., van Dam J., Crawford J.M., Manoharan R., Feld M.S. *IEEE Trans. Biomed. Eng.*, **43**, 113 (1996).
17. Marchesini R., Pignoli E., Tomatis S., Fumagalli S., Sichirollo A.E., Palma S.D., Fante M.D., Spinelli P., Croce A.C., Bottirollo G. *Lasers Surg. Med.*, **15**, 351 (1994).
18. Holmer C., Lehmann K.S., Risk J., Roggan A., Germer C.-T., Reissfelder C., Isbert C., Buhr H.J., Ritz J.-P. *Lasers Surg. Med.*, **38**, 296 (2006).

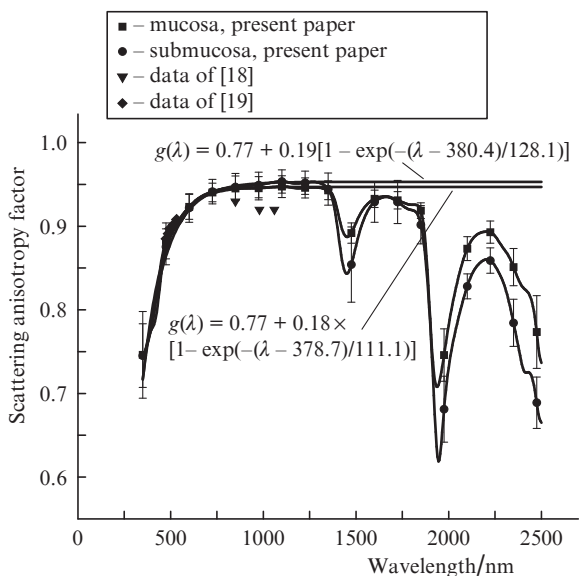


Figure 6. Scattering anisotropy factor of human colon tissue.

19. Wei H.-J., Xing D., Lu J.-J., Gu H.-M., Wu G.-Y., Jin Y. *World J. Gastroenterology*, **11**, 2413 (2005).
20. Prael S.A., van Gemert M.J.C., Welch A.J. *Appl. Opt.*, **32**, 559 (1993).
21. Wang L., Jacques S.L., Zheng L. *Comput. Methods & Programs Biomed.*, **47**, 131 (1995).
22. Bundy B. *Basic Optimization Methods* (Baltimore: Edward Arnold Publishers, 1984; Moscow: Radio i svyaz', 1988).
23. Kou L., Labrie D., Chylek P. *Appl. Opt.*, **32**, 3531 (1993).
24. Palmer K.F., Williams D. *J. Opt. Soc. Am.*, **64**, 1107 (1974).
25. <http://omlc.ogi.edu/spectra/hemoglobin/>.
26. Ishimaru A. *Wave Propagation and Scattering in Random Media* (New York: Academic, 1978) Vol. 1.
27. van Gemert M.J.C., Star W.M. *Lasers Life Sci.*, **1**, 287 (1987).
28. Groenhuis R.A.J., Ferwerda H.A., Ten Bosch J.J. *Appl. Opt.*, **22**, 2456 (1983).
29. Hidovic-Rowe D., Claridge E. *Phys. Med. Biol.*, **50**, 1071 (2005).
30. Terentyuk G.S., Ivanov A.V., Polyanskaya N.I., Maksimova I.L., Skaptsov A.A., Chumakov D.S., Khlebtsov B.N., Khlebtsov N.G. *Kvantovaya Elektron.*, **42** (5), 380 (2012) [*Quantum Electron.*, **42** (5), 380 (2012)].
31. Bohren C.F., Huffman D.R. *Absorption and Scattering of Light by Small Particles* (New York: Wiley, 1983; Moscow: Mir, 1986).
32. Du Y., Hu X.H., Cariveau M., Kalmus G.W., Lu J.Q. *Phys. Med. Biol.*, **46**, 167 (2001).
33. Ritz J.-P., Roggan A., Isbert C., Muller G., Buhr H., Germer C.-T. *Lasers Surg. Med.*, **29**, 205 (2001).
34. Fu Q., Sun W. *Appl. Opt.*, **40**, 1354 (2001).
35. Sun W., Loeb N.G., Lin B. *Appl. Opt.*, **44**, 2338 (2005).
36. Mourant J.R., Fuselier T., Boyer J., Johnson T.M., Bigio I.J. *Appl. Opt.*, **36**, 949 (1997).
37. Schmitt J.M., Kumar G. *Appl. Opt.*, **37**, 2788 (1998).
38. Wang R.K. *J. Modern Opt.*, **47**, 103 (2000).
39. Jacques S.L. *J. Innovative Optical Health Sci.*, **4**, 1 (2011).
40. Shchyogolev S.Yu. *J. Biomed. Opt.*, **4**, 490 (1999).